Journal of Applied Polymer Science

The nature of polymer grafts and substrate shape on the surface degradation of poly(L-lactide)

Robertus Wahyu N. Nugroho, Karin Odelius, Anders Höglund, Ann-Christine Albertsson
Department of Fibre and Polymer Technology, KTH Royal Institute of Technology, SE-10044, Stockholm, Sweden
Correspondence to: A.-C. Albertsson (E-mail: aila@kth.se)

ABSTRACT: Surface grafting of functional polymers is an effective method to alter material properties and degradation behavior. Two different substrate shapes of poly(L-lactide) (PLLA), i.e., films and microparticles, were surface-grafted with hydrophilic monomers, and their surface degradation was monitored. Surface grafting with a hydrophilic and acidic polymer graft [acrylic acid (AA)] induced large alterations in the surface morphology and topography of the films. In contrast, hydrophilic and neutral polymer grafts [acrylamide (AAm)] had no significant effect on the surface degradation behavior, while the PLLA reference and co-monomeric (AA/AAm) polymer-grafted samples exhibited intermediate surface degradation rates. The grafted PAA chains induced a local acidic environment on the surface of the substrates, which in turn catalyzed the surface degradation process. This effect was more pronounced in the films than in the microparticles. Thus, the nature of the grafted chains and substrate geometry were shown to affect the surface degradation behavior of PLLA substrates. © 2015 The Authors Journal of Applied Polymer Science Published by Wiley Periodicals, Inc. J. Appl. Polym. Sci. **2015**, *132*, 42736.

KEYWORDS: degradation; properties and characterization; surfaces and interfaces

Received 18 June 2015; accepted 15 July 2015
DOI: 10.1002/app.42736

INTRODUCTION

Surface modification of polymers is a powerful tool to induce changes in material properties.[1–4] The topography, chemistry, and physics of the surface are crucial parameters that affect the properties of the materials.[5–9] Surface-grafted polymers have been used in a variety of applications[10] for instance, cell adhesion promoters,[11,12] bio-functional coatings,[13–17] and surface stabilizers of colloids.[18,19] Polymers are for several reasons excellent candidates for surface modification: (1) a large number of specific functional groups can be created; (2) a wide variety of functional groups are available; and (3) they serve as multifunctional stimuli-sensitive materials.[20] In addition, surface modification has previously been used as a tool to tune the degradation rate of biodegradable polymers, for instance, poly(L-lactide) (PLLA).[21–24] We have previously shown that surface modification with acrylic acid (AA) changes the bulk degradation behavior of PLLA.[23] Short and long AA-grafted lactic acid oligomers as well as plain lactic acid oligomers were detected in the degradation media. The presence of at least one lactic acid monomer in each released degradation product confirmed the hydrolysis of the PLLA substrate. A second alternative for surface-grafted polymers is the detachment of the grafted chains alone, which may occur when side-chain densities of the polymer grafts are quite high and polymer–surface interactions are sufficiently unfavorable.[25,26] Hydrophilic brushes prepared by surface-initiated atom transfer radical polymerization were shown to detach from glass substrates with high chain densities.[14] In addition, swelling-induced detachment of hydrophilic grafts from hydrophobic substrates has also been demonstrated.[27] The dynamics of such phenomena have also been investigated theoretically[28] and by mathematical models via Monte Carlo simulations.[29] The grafted chains could also be mechanically detached using a very weak applied force. Thus, for mechanical detachment the applied force depends on the surface, polymer, and solvent.[30,31] Despite the large efforts in surface modification of polymers, less attention has been paid to the degradation of the surface-grafted polymers and, perhaps more importantly, the nature of different surface-grafted chains and substrate geometry on the degradation behavior.

PLLA is well known to degrade by bulk erosion. The degradation mechanism is hydrolysis of the ester bonds in the main chain. Cleavage of ester bonds results in the formation of acidic groups, which were earlier shown to catalyze further degradation.[32] In previous work, surface modification with hydrophilic

Additional Supporting Information may be found in the online version of this article.

AA was used to increase the bulk degradation rate of hydrophobic PLLA.[23] Here, we aim to take advantage of this effect by creating a localized acidic environment in the vicinity of the grafts. Our hypothesis is that the nature of the grafts should play an important role in the early stage of degradation of surface-grafted microparticles and that acid-grafted films should be affected earlier during degradation than acid-grafted microparticles.

Thus, films and microparticles of PLLA were surface-grafted with AA, neutral acrylamide (AAm) and a combination of both monomers using a nondestructive covalent "grafting-from" technique described previously.[33] The samples were subjected to hydrolytic degradation for up to 30 days to determine the influence of surface grafts and sample morphology.

EXPERIMENTAL

Materials

PLLA was synthesized by ring-opening polymerization of L-lactide (LLA, Boehringer Ingelheim, Germany) at 110°C for 72 h in bulk, using ethylene glycol (Aldrich, Germany) as the initiator and stannous octoate ($(Sn(Oct)_2$)(Sigma Aldrich, Sweden) as the catalyst. The formed polymer was precipitated three consecutive times in cold hexane (LabScan, Ireland)/methanol (general purpose grade, Fisher Scientific, Germany). AA (90%, Alfa Aesar) was purified by vacuum distillation at 40–50°C prior to use. Benzophenone (BP) (99%, Sigma Aldrich), AAm (98.5%, Acros), and PBS buffer (VWR) were all used as received.

Film and Microparticles Fabrication

For the film substrates, a predetermined amount of PLLA (1.5 g) was dissolved in chloroform (36.5 g), stirred until a homogenous solution was formed, and then poured into a Petri dish from which the organic solvent was allowed to slowly evaporate. For the microparticulate substrates, 1% (w/v) solution of PLLA in chloroform was prepared. PLLA microparticles were then fabricated using a spray dryer (Mini Spray Dryer BÜCHI B-290, Flawill, Switzerland). The following system parameters were used: inlet temperature (T_{inlet}) 55–65°C, aspirator 100% (35 m^3/min), pump feed rate 20%, gas flow 50 mm (750 Nl/h). The dried microparticles were then recovered in a collecting device located beneath the spray drying cyclone.

Surface Grafting of Films and Microparticles

PLLA films were punched to obtain uniform samples with an approximate mass of 22 ± 2 mg and a circular shape 1 cm in diameter and 0.22 mm in thickness. The PLLA films and microparticles were subsequently surface-grafted with 20% (w/v) AA, AAm, and AA/AAm with a volume ratio of 1:1 under UV irradiation, as previously described.[33] The films and microparticles were grafted for 1.5 h. The grafted films and microparticles were recovered and rinsed several times with ethanol under 5000 G centrifugation for 3 min to remove unreacted monomers. Neat PLLA films and microparticles, used as reference, were also treated with the same procedures, but without the addition of monomers.

Surface Degradation Studies

For particulate PLLA samples, a predetermined amount of surface-grafted microparticles (approximately 20–25 mg) were placed in a dialysis bag. The circular-shaped PLLA films and dialysis bags containing PLLA microparticles were placed in individual 20 mL glass vials containing 10 mL of PBS buffer at pH 7.4 and subsequently tightly closed with septa. The vials were put in a controlled incubator at 37°C and shaken at a rotational velocity of 60 rpm. At predetermined time intervals (5, 10, 14, and 30 days); the samples were taken out of the shaking incubator. The samples were finally dried under vacuum until they reached a constant mass and were subsequently characterized.

Characterization

Scanning Electron Microscopy. The surface morphology of the neat and grafted PLLA films and microparticles was observed with a Hitachi S-4800 scanning electron microscope (SEM) at an accelerating voltage of 1 kV. The samples were mounted on adhesive carbon black and sputter-coated.

Fourier Transform Infrared (FTIR) Spectroscopy. Fourier Transform Infrared (FTIR) spectra of the neat and grafted PLLA films and microparticles were recorded in the range of 4000–600 cm^{-1} on a Spectrum 2000 Perkin-Elmers spectrometer, equipped with an attenuated total reflectance (ATR) accessory (Golden Gate) to provide surface analysis to a depth of approximately 1 μm. All FTIR spectra were obtained as averages of 16 individual scans at 4 cm^{-1} resolution.

Atomic Force Microscopy. The surface topography of the neat and grafted PLLA films and microparticles were examined in tapping mode using a Nanoscope IIIa multimode Atomic Force Microscopy (AFM) (Digital Instruments, Santa Barbara, CA) using a 5346 EV scanner. A silicon-etched probe tip (TAP150, Bruker, Camarillo, CA), with a normal spring constant of 5 N/m and a resonant frequency (f_o) of 150–200 kHz, was utilized to scan the image in tapping mode.

Differential Scanning Calorimetry. The thermal properties of the neat and grafted PLLA films and microparticles were examined by differential scanning calorimetry (DSC) (Mettler Toledo, Columbus, OH) equipped with DSC 820 software. The samples were weighed (approximately 3–5 mg) in 40 μL aluminum crucibles. They were then heated from −20°C to 200°C, cooled to −20°C and once again heated to 200°C using a heating/cooling rate of 10°C/min under a nitrogen atmosphere.

Mass Loss. The degradation was also monitored by measuring the samples' remaining mass after each hydrolysis period. After withdrawing the materials from the PBS buffer, they were dried under reduced pressure until constant weight was achieved. The remaining mass was determined according to the following equation:

$$\text{remaining mass} = \frac{m_d}{m_0} \times 100 \quad (1)$$

where m_d is the dry mass of the specimen at the specific time and m_0 is the initial mass of the specimen.

Size Exclusion Chromatography. The molar mass of the neat PLLA films and microparticles during degradation were determined using a Waters 717 Plus autosampler and a Waters 510 apparatus equipped with two PL gel 10 μm mixed B columns, 300 × 7.5 mm (Polymer Laboratories, U.K). Chloroform was used as an eluent at a flow rate of 0.1 mL/min. The instrument was calibrated using narrow molar mass distribution polystyrene standards with molar masses in the range 580–400,000 g/mol.

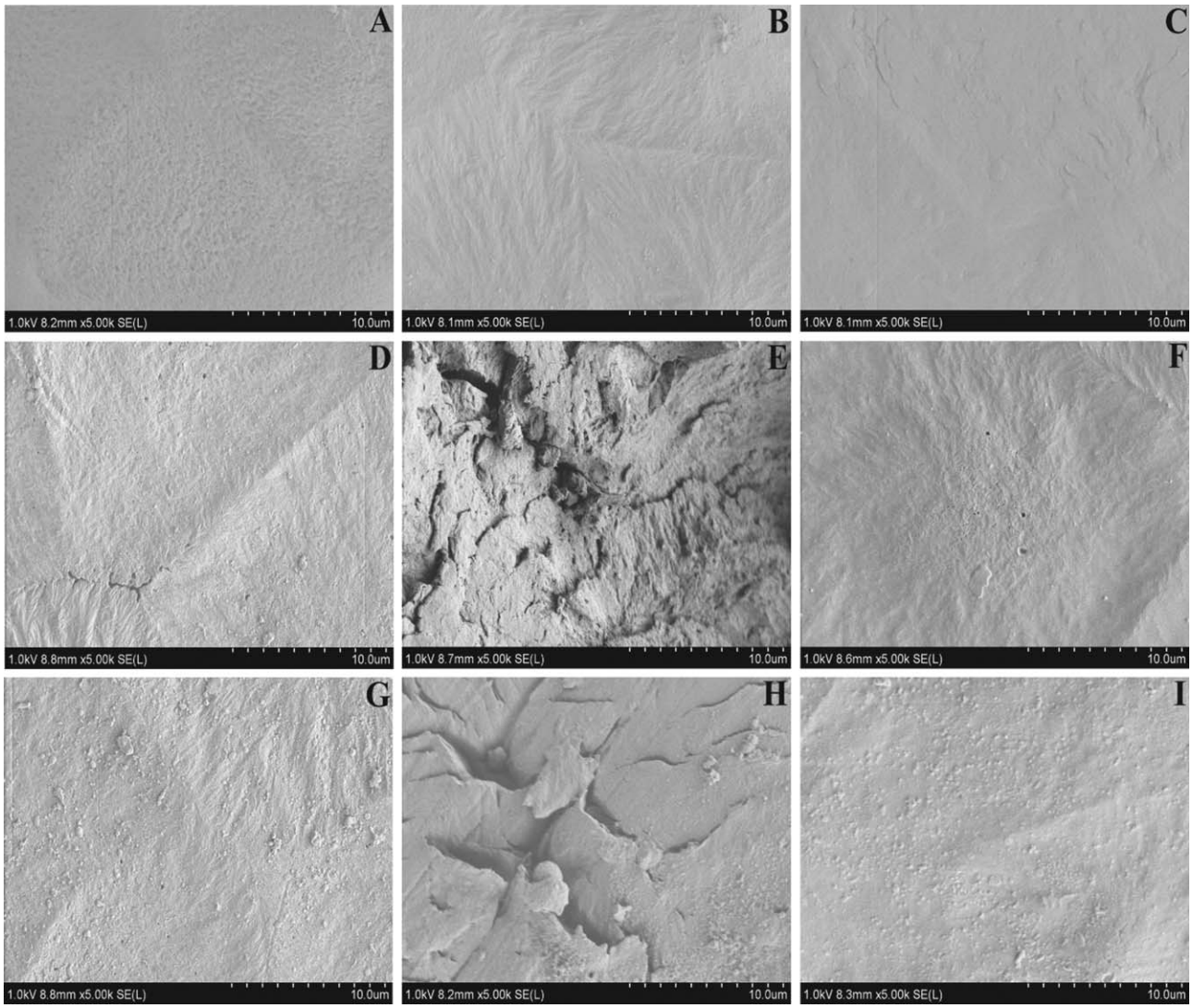

Figure 1. Surface morphologies of films of (**top**): (A) PLLA, (B) PLLA-g-PAA, and (C) PLLA-g-PAAm at day 0; (**middle**): (D) PLLA, (E) PLLA-g-PAA and (F) PLLA- g-PAAm at day 14; (**bottom**) (G) PLLA, (H) PLLA-g-PAA and (I) PLLA- g-PAAm at day 30.

pH Measurement. The pH of the surface degradation media was evaluated using a precalibrated pH-meter equipped with an Ag/AgCl electrode.

RESULTS AND DISCUSSION

Two different PLLA substrates, films and microparticles, were prepared and surface-grafted with AA, AAm, and AA/AAm (1 : 1). The degradation behavior of the grafted substrates and a PLLA reference was evaluated after immersion in PBS buffer at a pH of 7.4 for up to 30 days. From the results obtained, it could be determined that the nature of the polymer grafts altered the degradation behavior of sample surfaces and depending on the grafted substrate geometry, degradation occurred at different times during PBS immersion. This could be determined by investigating the surface morphology, surface chemistry, surface topography, thermal properties, mass loss, and pH profiles.

Surface Morphologies of Films and Microparticles Substrates

In general, much larger alterations in the surface morphology were found for the films (Figure 1) compared to the microparticles (Figure 2) as a function of degradation time. Prior to surface degradation, the surface of PLLA-based films had a smooth morphology [Figure 1(A–C)] and neat PLLA film had slightly porous structures because of solvent evaporation during film fabrication [Figure 1(A)]. Surface degradation was especially evident for the PLLA-g-PAA films, where large cracks appeared after 10 days of degradation [Figure 1(E)] and then remained evident throughout the study [Figure 1(H)]. For the neat PLLA films, a small number of microcracks were formed on the surface after 14 days of degradation [Figure 1(D)] and after 30 days of degradation (1G), while the PLLA microparticles retained the same surface morphology before [Figure 2(A)], during [Figure 2(D)], and even after a month of degradation [Figure 2(G)]. Similar to the neat PLLA microparticles, the surface morphology of both substrates with PAAm grafts remained unaltered even after 30 days of degradation [Figure 1(I)]. For

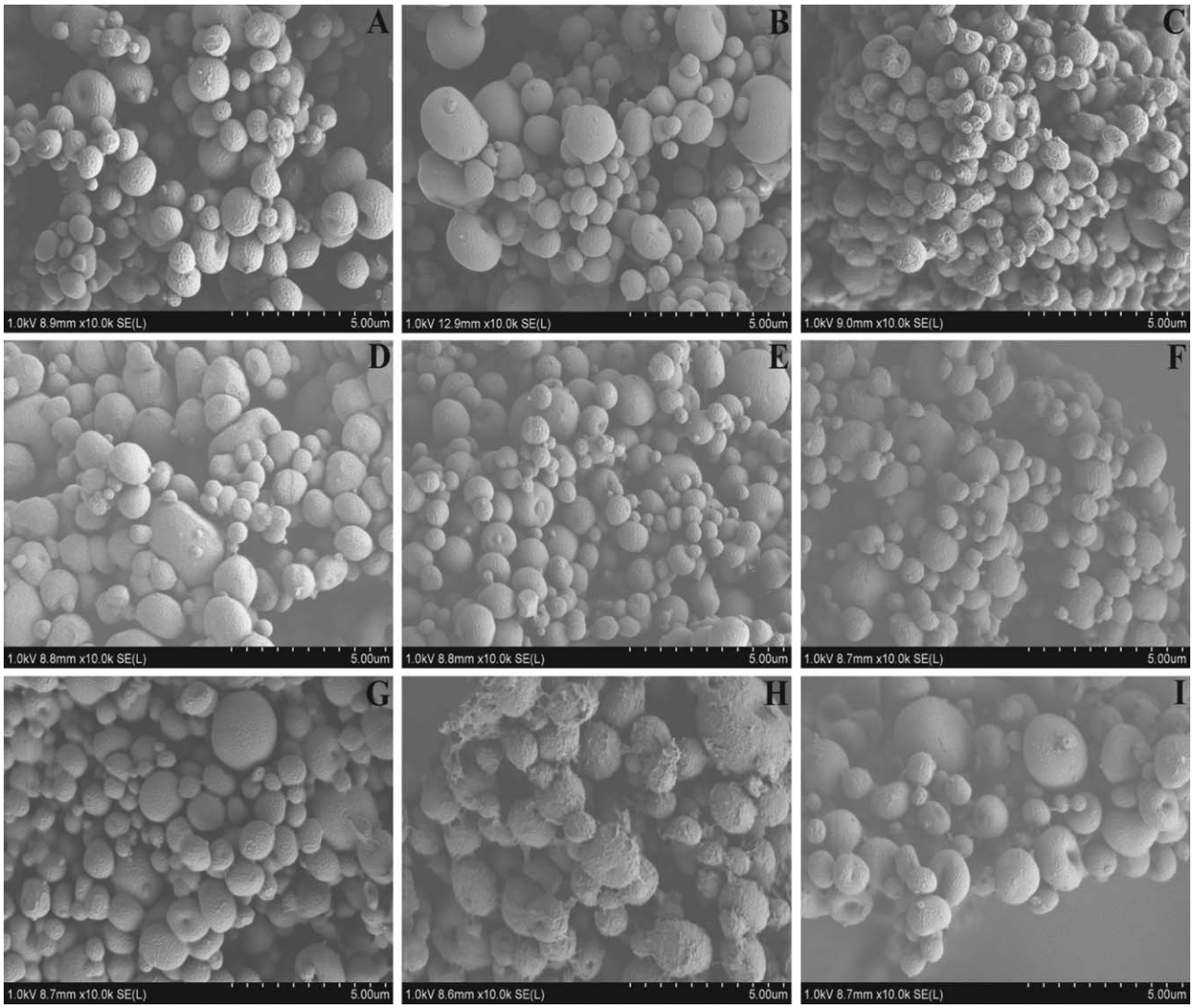

Figure 2. Surface morphologies of microparticles of (**top**): (A) PLLA, (B) PLLA-g-PAA, and (C) PLLA-g-PAAm at day 0; (**middle**): (D) PLLA, (E) PLLA-g-PAA and (F) PLLA- g-PAAm at day 14; (**bottom**) (G) PLLA, (H) PLLA-g-PAA and (I) PLLA- g-PAAm at day 30.

the polymer grafts where a combination of AA and AAm was used, small alterations in the surface morphology of the films were seen after 14 days of immersion (formation of micro cracks) (Supporting Information Figure S3B), while the microparticles showed a slightly altered surface morphology after 30 days of degradation (Supporting Information Figure S4C).

As previously stated, the surface morphology of the PLLA-g-PAA films was greatly affected by the immersion in PBS at a pH of 7.4. Already after 10 days of immersion, large cracks were seen on the surfaces [Figure 1(E)]. To investigate if the formation of these large cracks was a result of the actual grafting of PAA to the backbone of PLLA or only a consequence of the more acidic environment formed because of the presence of PAA, neat PLLA films were also immersed in two different concentrations of PAA, i.e., 0.3% (w/w), yielding a pH of 6.9, and 3% (w/w), yielding a pH of 5.0 in PBS. It should be noted that the concentrations of PAA in PBS used greatly exceeded the possible amount of PAA covalently grafted to the PLLA films, and the high concentrations were chosen in order to conclusively answer our question of whether the covalent attachment of PAA is the key issue. We have, as of now, not been able to determine the exact amount of PAA covalently grafted to the PLLA films. However, from a similar previous study,[34] the maximum amount of grafted chains to the substrates was lower than the smallest amount of dissolved PAA in the PBS solution. At a higher pH, the acid groups of the PAA chains ionize, releasing aqueous H^+ cations. It is well known that the acidic end-groups formed during the degradation of PLLA lead to an autocatalytic effect and hence a faster degradation of the PLLA main chain.[32] The neat PLLA films and microparticles were incubated in the solutions for 14 and 30 days, respectively. No alterations of the surface morphology were observed for the PLLA films, even at day 30 of immersion in the highly acidic solution (Supporting Information Figure S1). This is contrary to what was seen for the films onto which PAA was covalently attached, in which large cracks were observed already after 10 days of immersion [Figure 1(E)]. The reason for the difference between the PLLA-g-PAA films and

the PLLA films in a PAA solution (that were treated in an identical manner as the grafted films without the addition of the monomer) is thus believed to be because of the covalent attachment of the grafts and thereby created localized acidic environment. A hypothesis is that the hydrophobic PLLA matrix might suppress the swelling behavior of the PAA grafts in the PBS solution. The mechanical stress resulting from the osmotic pressure of the PAA grafts is then localized on the hydrophobic matrix (crystallites), leading to swelling-induced surface erosion of the substrates. This effect would be much larger for PAA grafts compared to the PAAm grafts, because of PAA showing much more pronounced swelling behavior than PAAm.[27,35]

For the PLLA films grafted with a combination of AA and AAm, alteration of the surface morphology was observed after 14 days of degradation (Supporting Information Figure S3B), which occurred later compared to the PLLA-g-PAA films [Figure 1(E)]. This retardation of surface degradation is believed to be a consequence of the lower amount (ca. 50% volume) of AA grafted to the PLLA surface and hence the less acidic surface environment (Supporting Information Figures S3B and S3C).

As stated above, no alteration to the surface morphology of the neat PLLA microparticles [Figure 2(A,D,G)] and the PLLA-g-PAAm microparticles was observed throughout the duration of the degradation study [Figure 2(C,F,1)]. Similar to the films, differences in the surface morphology were seen when PAA was grafted to a PLLA matrix. However, the surface morphological changes were not in the form of large cracks as they were for the films, but rather in the form of a rougher surface, and they did not occur after 14 days [Figure 2(E)], but at a later time point (30 days of immersion) [Figure 2(H)]. To evaluate here as well if this was an effect of grafting or because of an increased acidic environment, neat PLLA microparticles were immersed in 0.3% (w/w) and 3% (w/w) solutions of PAA in PBS. No alterations in the surface morphology could be determined for the neat PLLA microparticles (Supporting Information Figure S2); hence, it is believed that it is the covalent attachment of the chains that alter the surface degradation of the microparticles. Once again, the degradation of the surface was retarded for the PLLA–g-PAA/PAAm microparticles compared to their film analogues. It can thereby be concluded that the substrate shape plays a key role in the alteration of surface morphology for the PLLA matrices grafted with hydrophilic monomers. For the microparticles whose surface morphologies were observed to change, these changes occurred at a later time point compared to the film substrates. Additionally, the nature of the polymer grafts plays an essential role in the degradation behavior. The localized acidic environment formed when AA was surface-grafted to the substrate induced earlier changes in the surface morphology of the substrates than in both the neat PLLA and substrates grafted with PAAm. In contrast, when AAm was grafted on the surface, no change in surface morphology of the substrates was observed within the time of the study, indicating a retardation of degradation. When a mixture of AA and AAm was surface-grafted to the substrates, intermediate behavior was observed. A plausible explanation is that although the hydrophilic grafts have a larger affinity for water than the PLLA substrate, increased hydrophilicity is not enough to increase the rate of change in surface morphology within 30 days of PBS immersion. The nature of the polymer grafts and hence the surface local environment they induce can control the surface degradation, as shown in the relative degrees of surface alterations: PLLA-g-PAA>PLLA, PLLA-g-PAA/PAAm>PLLA-g-PAAm.

Surface Chemistries of Films and Microparticles Substrates

The surface chemistry of the grafted films and microparticles was evaluated using FTIR (Figure 3). Because the alterations in the surface morphology depended on both the geometry of the substrate and degradation time, a comparison was made based on substrate geometry as a function of time. Again and as expected, no significant alterations were seen for the PLLA reference as a function of degradation time [Figure 3(A)].[23] Because the characteristic ester –C=O bands for the PLLA-g-PAA overlapped at approximately 1747 cm^{-1}, no changes in surface chemistry could thus be determined when the samples were immersed in PBS from day 0 to day 30 [Figure 3(D)].

When AAm was grafted on the PLLA surfaces, double peaks or "bumps" were observed after 1.5 h of grafting, showing the characteristic primary amide band at 1660 cm^{-1} and the stretching vibrations of the secondary amide band at the absorbance peak of 1615 cm^{-1} [Figure 3(B)].[33] The substrate geometry was shown to influence the surface grafting process, where more PAAm was attached to the films than to the microparticles, leading to a larger amide peak area for the films (peak area $\sim$ 6 A/cm) than that for the microparticles (peak area $\sim$ 3 A/cm). In contrast, when the two different geometries were surface-grafted with AA/AAm (1:1), the peak area was much larger for the microparticles (peak area $\sim$ 7 A/cm) than for the films (peak area $\sim$ 3 A/cm) [Figure 3(E)]. After 5 days of PBS immersion, the amount of PAAm grafted to the chains decreased significantly for both substrates [Figure 3(E)]. An approximate reduction of 40% was seen for the PLLA-g-PAAm films, while a 60% reduction was seen for the PLLA-g-PAAm microparticles [Figure 3(F)]. Although the peak area of the PAAm grafts was reduced so significantly after just 5 days of immersion, the surface morphology of the two substrates was not effected [Figures 1(I) and 2(I)]. Between 14 and 30 days of degradation, the amount of PAAm detected by FTIR on the microparticles was unchanged, whereas the amount of PAAm on the films continued to decrease. The surface degradation of PAAm continued until day 30 of degradation where approximately 16% (peak area $\sim$ 1 A/cm) was retained for the films and 24% (peak area $\sim$ 0.8 A/cm) was retained for the microparticles [Figure 3(E)]. At day 30, the peak area of the PAAm chains was larger for the microparticles than the films, which might have been because of a higher density of grafted chains as they were being compressed against each other; the IR spectrum was thus able to detect their existence. Once again, the grafted chains behaved differently depending on how they interacted on different substrates. After 10 days of immersion, the microparticles seemed to lose more grafted chains from their surfaces [Figure 3(E)]. There are two possible driving forces, i.e., entropic elastic and osmotic,[36,37] that play a critical role in compression and seem to reach a state of equilibrium, ultimately balancing each other. Most likely, the phenomenon is more complex when two monomers are used, i.e., AA and

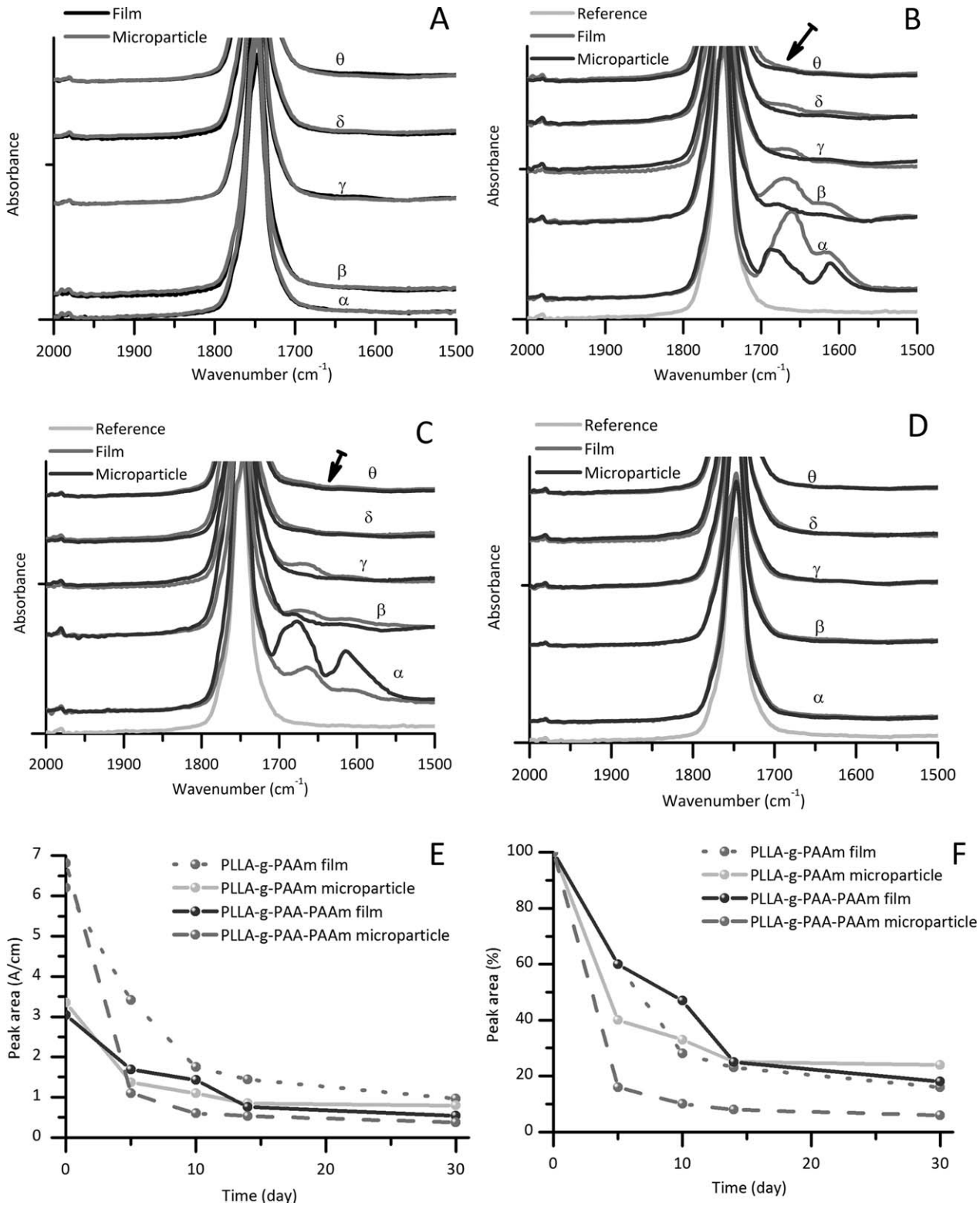

Figure 3. ATR-FTIR spectra of films and microparticles of (A) PLLA (B) PLLA-g-PAAm, (C) PLLA-g-PAA/PAAm, (D) PLLA-g-PAA, (E) and (F) peak area of PAAm and PAA/PAAm in A/cm and in percentage, respectively, at 1550–1700 cm^{-1} for immersion times of 0 (α), 5 (β), 10 (γ), 14 (δ) and 30 (θ) days.

AAm. The IR spectra of the microparticles surfaces grafted with AA/AAm [Figure 3(C)] showed similar results to AAm-only grafting [Figure 3(B)], where the grafted chains detached much faster from the microparticle surfaces than from the films from day 5 onward. However, the presence of AA/AAm deeply impacted the stability of grafted chains on PLLA microparticles,

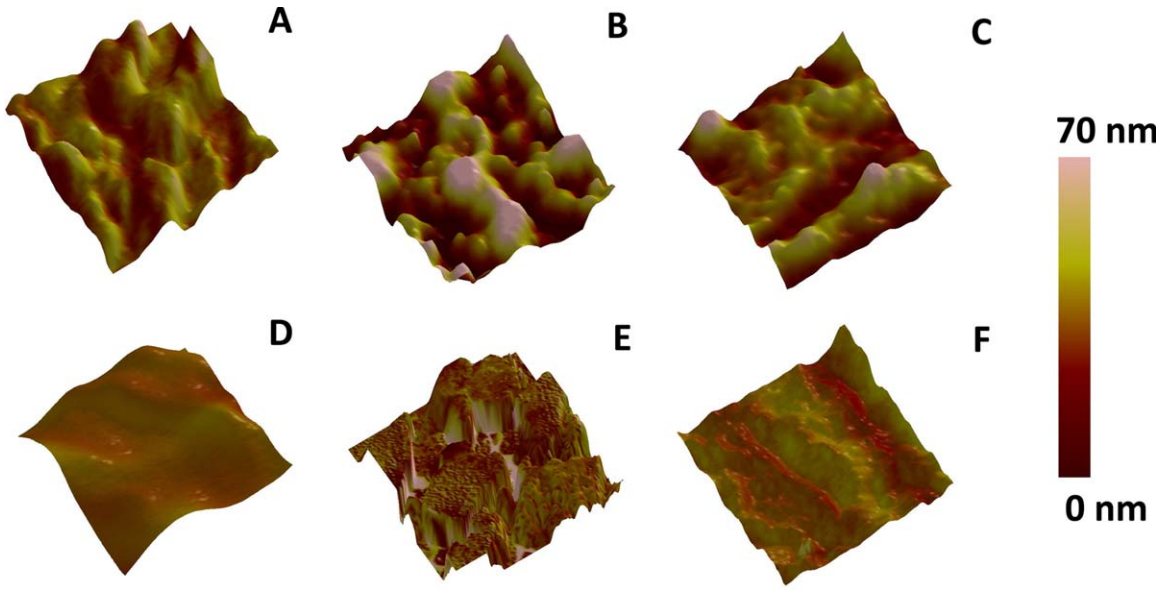

Figure 4. AFM 3D-images of the surface topography of films of (**top**): (A) PLLA, (B) PLLA-g-PAA (C) PLLA-g-PAAm at day 0; (**bottom**) (D) PLLA, (E) PLLA-g-PAA, (F) PLLA-g-PAAm at day 30. All AFM images were scanned over an area of 2 μm × 2 μm. [Color figure can be viewed in the online issue, which is available at wileyonlinelibrary.com.]

and approximately 20% of the AA/AAm grafted chains were still attached to the surface of microparticles, whereas 40% of AAm-based polymer grafts were retained [Figure 3(F)]. This might have been because of a slightly higher osmotic stress caused by the combination of monomers; the interactions between them might cause the polymer grafts to be stretched beyond their physical limits, leading to more abundant surface degradation of the polymer grafts [Figure 3(C)].

The difference in the alterations in the surface chemistry of the microparticles compared to the films could have several causes. One reason could be the fact that a fraction of the grafted chains that were entangled or adsorbed to the substrate surface was released upon prolonged water immersion and that more chains were noncovalently attached to the microparticle surfaces because of the larger surface area compared to the films. The difference could also be explained by a higher osmotic pressure

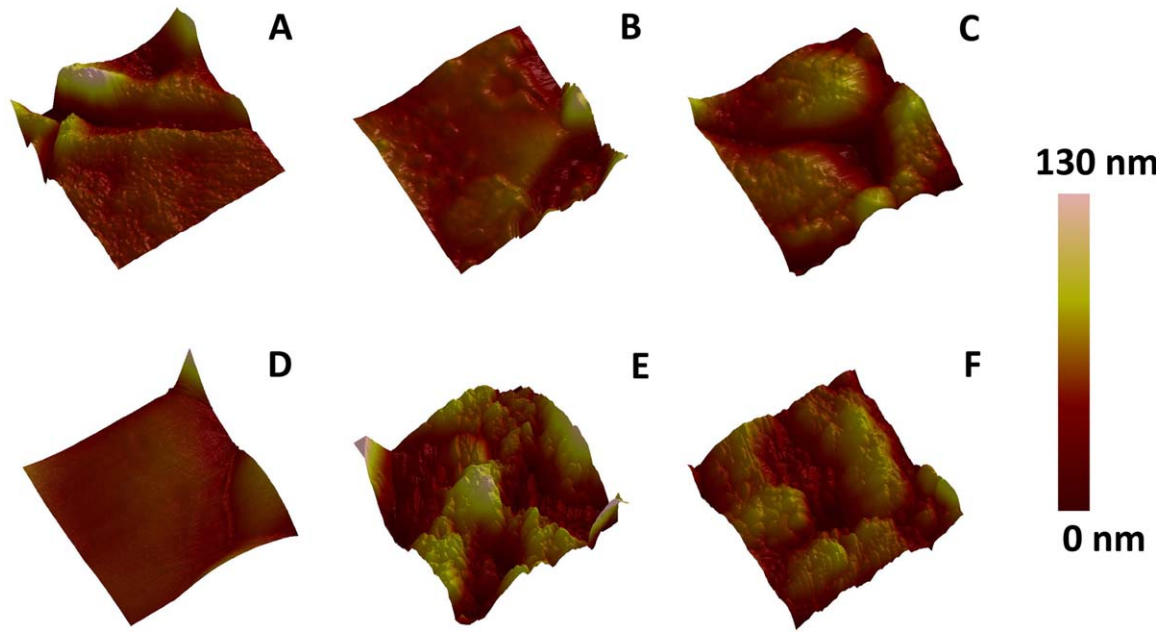

Figure 5. AFM 3D-images of the surface topography of microparticles of (**top**): (A) PLLA, (B) PLLA-g-PAA (C) PLLA-g-PAAm at day 0; (**bottom**) (D) PLLA, (E) PLLA-g-PAA (F) PLLA-g-PAAm at day 30. All AFM images were scanned over an area of 800 nm × 800 nm. [Color figure can be viewed in the online issue, which is available at wileyonlinelibrary.com.]

Table I. Surface Roughness of PLLA Films and Microparticles during Surface Degradation at Day 0 and 30

	Surface roughness (nm)[a]			
	Films Time (day)		Microparticles Time (day)	
Sample	0	30	0	30
PLLA	21±1	16±5	30	7
PLLA-g-PAA	22	125±20	2	27
PLLA-g-PAAm	6	11±1	14	16±1

[a] Calculated from image area of 800 nm x 800 nm.

induced by the neighboring grafted microparticles when the grafted chains were being compressed at the beginning of PBS immersion.

Although the FTIR spectra indicated that a relatively low amount of polymer grafts remained after 30 days of immersion for both substrates, a grafted layer of PAAm still existed. Previously, when PLLA film substrates were grafted with PAA, the films could be dissolved in chloroform and the molar mass of the films could subsequently be determined by Size Exclusion Chromatography (SEC).[23] Here, even though the FTIR spectra showed a very low amount of PAAm still covalently attached to the substrates after 30 days of immersion, the films and microparticles could not be dissolved. However, the neat PLLA reference films (treated in the same manner as the grafted substrates but without the addition of monomers) could easily be dissolved in chloroform. This indicates that the layer of PAAm after 30 days of immersion is still significant enough to prevent dissolution and that the prevention of dissolution is not an effect of cross-linking reactions.

Surface Topographies of Films and Microparticles

To gain further insight into the degradation behavior of the grafted PLLA substrates, the surface topographies before and after 30 days of PBS immersion were evaluated (Figures 4 and 5). Depending on the nature of the polymer grafts and the geometry of the substrates, the degradation behavior again differed. For the grafted samples, a larger increase in surface roughness was seen in the films over time compared to the microparticles, and once again, a larger impact on the surface topography was seen when AA was grafted compared to when AAm was used. Generally for the PLLA substrates, the surface

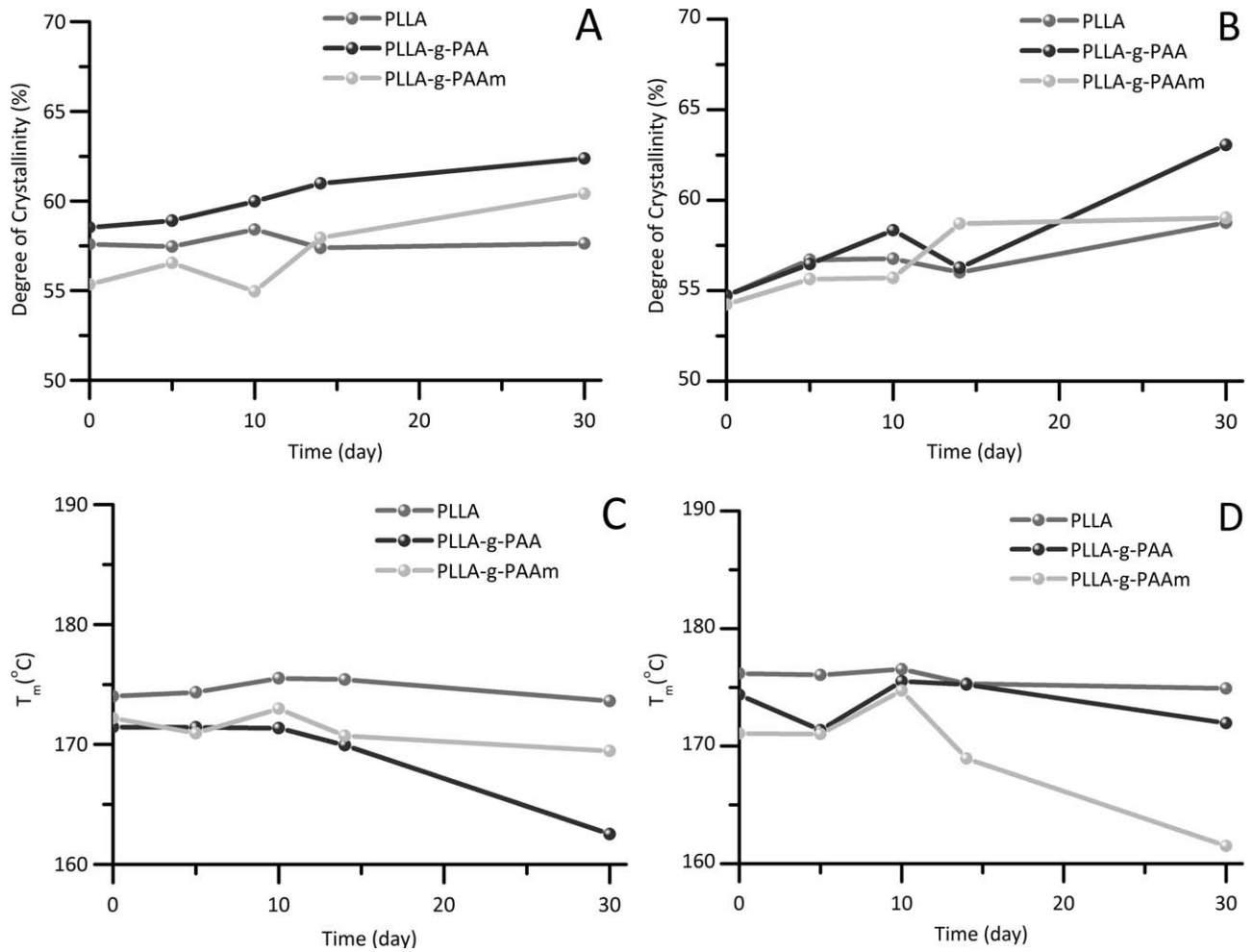

Figure 6. Degree of crystallinity of (A) films and (B) microparticles (**top**); melting temperature of (C) films and (D) microparticles (**bottom**) as a function of degradation time.

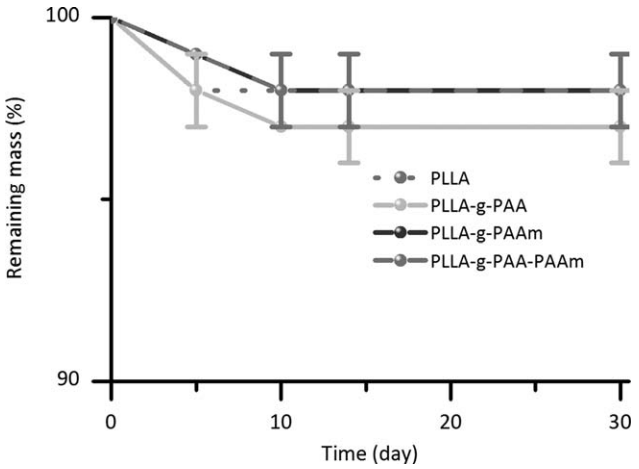

Figure 7. Remaining mass of polymeric films as a function of degradation time.

roughness decreased leading up to 30 days of degradation, while the opposite trend was seen for the grafted substrates. The largest alteration in roughness was seen for the PLLA-g-PAA films, which also showed the largest alteration of surface morphology (Figure 1), forming large cracks already after 10 days of degradation.

Initially, the PLLA film had a rough surface with an average rms roughness of 21 nm [Figure 4(A)] after UV irradiation in ethanol. The roughness of the PLLA films decreased after they were immersed in PBS solution for 30 days to an average rms roughness of 16 nm [Figure 4(D)]. The same roughness pattern was observed for microparticles, where a rougher surface was initially seen with an average rms roughness of 30 nm [Figure 5(A)] followed by a much more pronounced decrease to 7 nm after 30 days of PBS immersion [Figure 5(D]. When AA was surface-grafted on the substrates of different geometries, the resultant surfaces acquired distinctly different surface roughnesses (Table I). The surface of the microparticles became smoother, with an rms of 2 nm [Figure 5(B)], while the films attained a roughness similar to that of the PLLA surface after UV exposure [Figure 4(B)]. After 30 days of immersion, a 13-fold rougher surface was measured for the microparticles, while six-fold rougher surfaces were observed in films compared to their initial values. It is worth noting that PLLA-g-PAA film had the highest surface roughness among all PLLA-based films after PBS incubation.

The surface roughness of the PLLA-g-PAAm films and microparticles before immersion in PBS demonstrated the opposite trends in roughness, i.e., a decrease in roughness and hence smoother surfaces, compared to the surfaces grafted with AA, indicating a thicker grafted layer. Additionally, the surface roughness did not change significantly for the microparticle substrates, as measured for day 30 of immersion [Figure 5(F)], while a two-fold rougher surface was observed for PLLA-g-PAAm films [Figure 4(F)]. These results are thus consistent with the alterations of the surface morphology, where the PAA chains because of their pH sensitivity, and hence the formation of a localized acidic environment, eroded the surface of the film [Figure 1(E and H)] and roughened the surfaces of microparticles after PBS immersion [Figure 2(H)].

Thermal Analysis of Films and Microparticles

Somewhat similar to the surface morphologies, chemistries, and topographies, the thermal behavior also varies with the nature of the polymer grafts and geometries of the substrates (Figure 6). The crystallinity and melting temperatures of the PLLA films were not altered during the surface degradation study [Figure 6(A, C)], similar to what has been seen before,[38] while an increase in crystallinity was seen for the PLLA microparticles [Figure 6(B)], as determined from the second heating scan. During the fabrication process, the two different geometries experienced different physical environments, i.e., film casting and spray drying, that induce different crystal rearrangements of the polymers. For example, for the microparticles, the evaporation rate of the drying process influenced crystallization because it is a time-dependent process.[39,40]

For the surface-grafted films [Figure 6(A)] and microparticles [Figure 6(B)], an increase in the crystallinity of the PLLA substrate as a function of time because of recrystallization was observed. This increase in crystallinity of the grafted substrates was followed by a gradual decrease in melting temperature for both substrates after 10 days of immersion. Again, the nature of

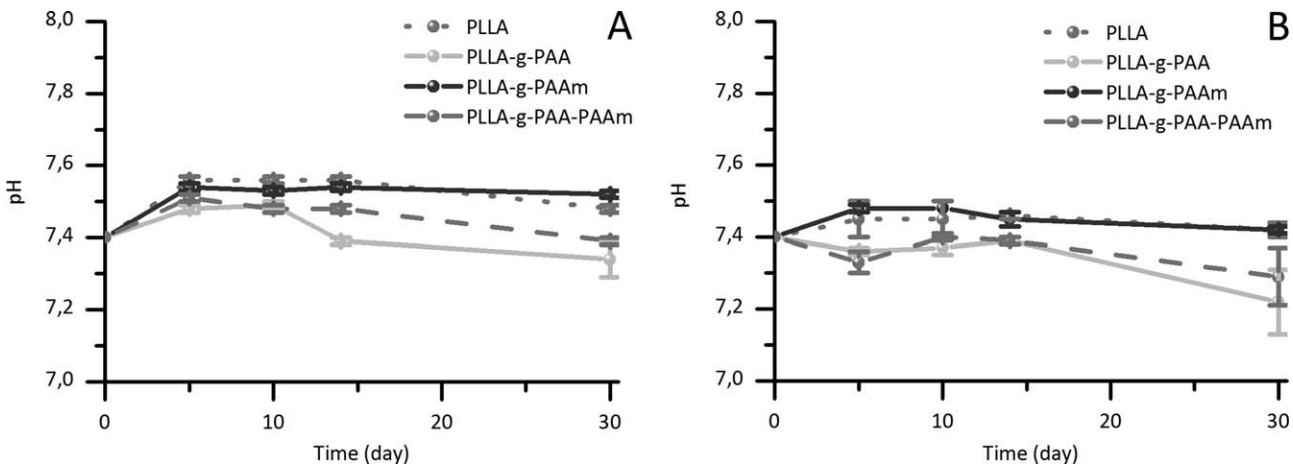

Figure 8. pH of media, in which (A) films and (B) microparticles were immersed, for different durations of surface degradation.

Table II. Molar Mass of PLLA Films and Microparticles before and after Different Durations of Surface Degradation

	Molar Mass (Mn).(g.mol^{-1})[a]			
	Film		Microparticle	
Time (day)	PLLA	$Đ_M$[a]	PLLA	$Đ_M$[a]
0	124,000	1.2	123,000	1.2
5	132,000	1.2	144,000	1.1
10	129,000	1.1	122,000	1.1
14	126,000	1.2	127,000	1.1
30	122,000	1.1	126,000	1.1

[a] Determined by SEC analysis (polystyrene standards for calibration and chloroform as an eluent).

the graft had an effect on the properties of the materials. The PLLA-g-PAA film exhibited a more pronounced decrease in melting temperature [Figure 6(C)] compared to the PAAm-grafted PLLA, while the opposite trend was seen for the microparticles [Figure 6(D)].

Mass Loss, Molar Mass Alterations, and pH Profiles

As expected, small changes in mass loss (Figure 7) were observed during the 30 days of surface degradation,[38] although significant changes in morphology, topography, and surface chemistry were observed for PLLA-g-PAA and PLLA-g-PAAm. PLLA-g-PAA films had a slightly faster mass loss rate because of the sensitivity of PAA at pH of 7.4, whereas PLLA, PLLA-g-PAAm, and PLLA-g-PAA/PAAm showed similar mass loss curves. For all samples, the mass loss occurred during early surface degradation and levelled off after 10 days. In addition, the presence of AA on the surfaces of films and microparticles obviously affected the pH of the media (Figure 8) as well as the morphological structures of these two geometrical substrates [Figures 1(H) and 2(H)].

As expected, no significant changes in molar mass were observed for the nongrafted materials during the 30 days of degradation (Table II). The grafted materials were not soluble in chloroform for SEC analysis, which confirmed that the grafting layers of PAAm or PAA remained attached to the substrate throughout the study. The molar mass of PLLA films and microparticles was the same as before UV treatment and substrate fabrication (Table II), confirming nondestructive fabrication techniques.

Again, both the nature of the polymer grafts and the substrate geometry affected the pH of the media as a function of immersion time. For the PLLA and PLLA-g-PAAm films, similar pH was measured from day 0 to 30 [Figure 8(A)], and no significant alterations in the samples' surface morphologies were observed for PLLA [Figure 1(G)] and PLLA-g-PAAm [Figure 11]. For the copolymeric grafts (PLLA-g-PAA/PAAm), an intermediate reduction in the pH of the medium over time was observed, similar to the intermediate alteration in surface morphology previously observed. In contrast, the pH of the PLLA-g-PAA medium decreased because of the presence of acrylic acid, which is in line with the observed differences in the surface morphology of the PLLA-g-PAA films [Figure 1(H)].

The trends in the pH of the different microparticulate PLLA samples were similar to the PLLA films [Figure 8(B)], although the pH of the media for the AA-grafted particles decreased slightly faster and at a higher rate. It is believed that the grafted chains might detach faster from the microparticles than from the films after day 5, as confirmed by FTIR, although a limited effect on the particle geometries at day 30 was observed [Figure 2(G–I)].

CONCLUSIONS

The nature of the grafted chains and substrate geometry were shown to affect the surface degradation behavior of PLLA. Surface degradation of AA-grafted PLLA films resulted in the formation of large cracks after 10 days of immersion, whereas AA-grafted PLLA microparticles resulted in a rougher surface formed after 30 days of immersion. The PAA grafted to the PLLA substrates induced a local acidic environment, which in turn catalyzed the surface degradation process. Larger alterations in the surface morphology were found in films than in microparticles. The surface morphology and topography of AAm-grafted PLLA films and microparticles were not affected during the time of the study, while films of co-monomeric (AA/AAm)-grafted PLLA exhibited an intermediate surface degradation rate. Hence, hydrophilicity alone is not enough to accelerate surface degradation.

The substrate geometry also affected the surface chemistry. PLLA microparticles surface-grafted with AAm degraded faster than the corresponding films, as confirmed by FTIR. Nevertheless, grafted chains remained on the surface of both geometries throughout the study.

In summary, surface morphology and surface chemistry are important factors to consider when functionalizing polymer substrates via surface grafting.

ACKNOWLEDGMENTS

The authors acknowledge the ERC Advanced Grant, PARADIGM (Grant Agreement No.: 246776) for the financial support of this work.

REFERENCES

1. Ogiwara, Y.; Kubota, H.; Hata, Y. *J. Polym. Sci. Polym. Lett. Ed.* **1985**, *7*, 365.
2. Deng, J.-P.; Yang, W.-T.; Rånby, B. *Macromol. Rapid Commun.* **2001**, *7*, 535.
3. Jianping, D.; Wantai, Y.; Rånby, B. *J. Macromol. Sci. A* **2002**, *8*, 771.
4. Zdyrko, B.; Luzinov, I. *Macromol. Rapid Commun.* **2011**, *12*, 859.
5. Anderson, J. M. *Annu. Rev. Mater. Res.* **2001**, *1*, 81.
6. Tirrell, M.; Kokkoli, E.; Biesalski, M. *Surf. Sci.* **2002**, 1, *61*.
7. Ratner, B. D.; Bryant, S. J. *Annu. Rev. Biomed. Eng.* **2004**, *1*, 41.

8. Liu, N.; Sun, G.; Gaan, S.; Rupper, P. *J. Appl. Polym. Sci.* **2010**, *6*, 3629.
9. Ishihara, K.; Kyomoto, M. *J. Photopolym. Sci. Technol.* **2010**, *2*, 161.
10. Yang, W.; Rånby, B. *Eur. Polym. J.* **1999**, *8*, 1557.
11. Källrot, M.; Edlund, U.; Albertsson, A.-C. *Biomaterials* **2006**, *9*, 1788.
12. Wong-In, S.; KhanhThuyen, N. T.; Siriwatwechakul, W.; Viravaidya-Pasuwat, K. *J. Appl. Polym. Sci.* **2013**, *5*, 3061.
13. Halperin, A. *Langmuir* **1999**, *7*, 2525.
14. Tugulu, S.; Klok, H.-A. *Biomacromolecules* **2008**, *3*, 906.
15. Drelich, J.; Chibowski, E.; Meng, D. D.; Terpilowski, K. *Soft Matter* **2011**, *21*, 9804.
16. Fristrup, C. J.; Jankova, K.; Hvilsted, S. *Soft Matter* **2009**, *23*, 4623.
17. Yang, W. J.; Neoh, K.-G.; Kang, E.-T.; Teo, S. L.-M.; Rittschof, D. *Prog. Polym. Sci.* **2014**, *5*, 1017.
18. Napper, D. H.; Netschey, A. *J. Colloid Interf. Sci.* **1971**, *3*, 528.
19. Wongthep, W.; Srituileong, S.; Martwiset, S.; Amnuaypanich, S. *J. Appl. Polym. Sci.* **2013**, *1*, 104.
20. Bhat, R.; Tomlinson, M.; Wu, T.; Genzer, J. In Surface-Initiated Polymerization II; Jordan, R., Ed.; Springer: Berlin Heidelberg, **2006**; Vol. *198*, p 51.
21. Peng, C.; Chen, H.; Wang, J.; Chen, Z.; Ni, M.; Chen, Y.; Zhang, J.; Yuan, T. *J. Appl. Polym. Sci.* **2013**, *1*, 704.
22. Källrot, M.; Edlund, U.; Albertsson, A.-C. *Biomacromolecules* **2007**, *8*, 2492.
23. Höglund, A.; Hakkarainen, M.; Edlund, U.; Albertsson, A.-C. *Langmuir* **2009**, *1*, 378.
24. Janorkar, A. V.; Metters, A. T.; Hirt, D. E. *Macromolecules* **2004**, *24*, 9151.
25. Deng, Y.; Zhu, X. Y. *J. Am. Chem. Soc.* **2007**, *24*, 7557.
26. Sheiko, S. S.; Sun, F. C.; Randall, A.; Shirvanyants, D.; Rubinstein, M.; Lee, H.-i.; Matyjaszewski, K. *Nature* **2006**, *7081*, 191.
27. Enomoto, K.; Takahashi, S.; Iwase, T.; Yamashita, T.; Maekawa, Y. *J. Mater. Chem.* **2011**, *25*, 9343.
28. Aubouy, M.; Harden, J. L.; Cates, M. E. *J. Phys. II France* **1996**, *7*, 969.
29. Binder, K.; Lai, P.-Y.; Wittmer, J. *Faraday Discuss.* **1994**, *0*, 97.
30. Alexander, M. S.; Leonid, I. K.; Alexey, A. P.; Kurt, B. *Europhys. Lett.* **2013**, *1*, 18003.
31. Zhang, W.; Zhang, X. *Prog. Polym. Sci.* **2003**, *8*, 1271.
32. Pitt, C. G.; Zhong-wei, G. *J. Control. Release* **1987**, *4*, 283.
33. Nugroho, R. W. N.; Odelius, K.; Höglund, A.; Albertsson, A.-C. *ACS Appl. Mater. Interfaces* **2012**, *6*, 2978.
34. Edlund, U.; Källrot, M.; Albertsson, A.-C. *J. Am. Chem. Soc.* **2005**, *24*, 8865.
35. Mohd Amin, M. C. I.; Ahmad, N.; Pandey, M.; Jue Xin, C. *Drug Dev. Ind. Pharm.* **2014**, *10*, 1340.
36. de Gennes, P. G. *Macromolecules* **1980**, *5*, 1069.
37. Witten, T. A.; Pincus, P. A. *Macromolecules* **1986**, *10*, 2509.
38. Höglund, A.; Odelius, K.; Albertsson, A.-C. *ACS Appl. Mater. Interfaces* **2012**, *5*, 2788.
39. Vehring, R. *Pharm. Res.* **2008**, *5*, 999.
40. Maa, Y.-F.; Costantino, H. R.; Nguyen, P.-A.; Hsu, C. C. *Pharm. Dev. Technol.* **1997**, *3*, 213.